Increasing the flexoelastic ratio of liquid crystals using highly fluorinated ester-linked bimesogens

PCCP

View Online / Journal Homepage
Dynamic Article Links

Cite this: DOI: 10.1039/c2cp43535g

www.rsc.org/pccp

PAPER

Increasing the flexoelastic ratio of liquid crystals using highly fluorinated ester-linked bimesogens

Katie L. Atkinson,[a] Stephen M. Morris,[a] Malik M. Qasim,[a] Flynn Castles,[a] Damian J. Gardiner,[a] Philip J. W. Hands,[a] Su Seok Choi,*[b] Wook-Sung Kim[b] and Harry J. Coles*[a]

Received 8th October 2012, Accepted 19th October 2012
DOI: 10.1039/c2cp43535g

We present experimental results on the bulk flexoelectric coefficients e and effective elastic coefficients K of non-symmetric bimesogenic liquid crystals when the number of terminal and lateral fluoro substituents is increased. These coefficients are of importance because the flexoelastic ratio e/K governs the magnitude of flexoelectro-optic switching in chiral nematic liquid crystals. The study is carried out for two different types of linkage in the flexible spacer chain that connects the separate mesogenic units: these are either an ether or an ester unit. It is found that increasing the number of fluorine atoms on the mesogenic units typically leads to a small increase in e and a decrease in K, resulting in an enhancement of e/K. The most dramatic increase in e/K, however, is observed when the linking group is changed from ether to ester units, which can largely be attributed to an increase in e. Increasing the number of fluorine atoms does, however, increase the viscoelastic ratio and therefore leads to a concomitant increase in the response time. This is observed for both types of linkage, although the ester-linked compounds exhibit smaller viscoelastic ratios compared with their ether-linked counterparts. Highly fluorinated ester-linked compounds are also found to exhibit lower transition temperatures and dielectric anisotropies. As a result, these compounds are promising materials for use in electro-optic devices.

1. Introduction

Flexoelectricity is a property displayed by all nematic liquid crystals (LCs).[1] Elastic deformation of the director field $\boldsymbol{n}$ can result in flexoelectric polarization $\boldsymbol{P}$ according to

$$\boldsymbol{P} = e_s\boldsymbol{n}(\nabla\cdot\boldsymbol{n}) + e_b\boldsymbol{n}\times(\nabla\times\boldsymbol{n}), \quad (1)$$

where e_s and e_b are the flexoelectric coefficients associated with splay and bend deformations, respectively, using the notation of ref. 2. For a chiral nematic LC, flexoelectric coupling results in a fast-switching electro-optic effect, in which the helical structure of the phase distorts when an electric field is applied perpendicular to the axis of the helix.[2] This leads to a macroscopic rotation of the optic axis. The effect is of particular interest because the response is considerably faster than that achievable in current displays based on nematic LCs. Specifically, rotation of the optic axis corresponding to full intensity modulation can occur within hundreds of microseconds, compared with conventional nematic LC displays, which respond in several milliseconds. Furthermore, this electro-optic effect is sufficiently fast for frame sequential colour.

From a device perspective it is important to understand how the macroscopic LC properties influence the electro-optic effect. Relationships for both the tilt angle of the optic axis and the response time have been derived elsewhere.[2,3] The flexoelectro-optic tilt angle ϕ for example, is related to the LC properties by[2]

$$\tan\phi = \frac{e}{K}\frac{p}{2\pi}E, \quad (2)$$

where K represents the effective elastic coefficient, which can be expressed in terms of the elastic coefficient for splay deformation K_1 and the elastic coefficient for bend deformation K_3 as $K = (K_1 + K_3)/2$ and e is the effective flexoelectric coefficient given by $e = (e_s + e_b)/2$. The ratio e/K is commonly referred to as the flexoelastic ratio. It can be seen that the tilt angle also depends on the pitch p of the helix and is linear in the applied electric field. For device applications, materials with a large e/K are required to achieve full intensity modulation at low electric field amplitudes.

The response time of the electro-optic effect is governed by a combination of the pitch and the visco-elastic properties. From a first order approximation, the response can be written as[3]

$$\tau = \frac{\gamma}{K}\frac{p^2}{4\pi^2}, \quad (3)$$

[a] *Centre of Molecular Materials for Photonics and Electronics, Department of Engineering, University of Cambridge, 9 JJ Thomson Avenue, Cambridge CB3 0FA, UK. E-mail: hjc37@cam.ac.uk*
[b] *LG Display, R&D Center, 1007, Deogeun-ri, Wollong-myeon, Paju-si Gyeonggi-do 413-811, Korea. E-mail: aiconess@lgdisplay.com*

where γ is the effective viscosity associated with the distortion of the helix and γ/K is referred to as the viscoelastic ratio. In this case it is clear that a short p and low γ/K are essential for fast switching of the optic axis.

As well as flexoelectric coupling, it is well known that chiral nematic LCs can interact with an electric field *via* dielectric coupling. In particular, the dielectric anisotropy $\Delta\varepsilon$ plays an important role in determining the critical electric field, at which the helical structure of the chiral nematic unwinds and flexoelectro-optic switching can no longer occur. Therefore, to extend flexoelectro-optic switching to high electric field amplitudes, materials with a low $\Delta\varepsilon$ are required.[2]

Overall, LC materials with properties that are optimized for flexoelectro-optic switching must have a short p, low $\Delta\varepsilon$, low γ/K, and large e/K. Conventional monomesogenic nematic LCs typically possess a low value for e and therefore exhibit relatively low values for e/K, which limits the usefulness of this effect for practical applications. As an example, measurements of the flexoelectric properties for the monomesogen 7OCB dispersed with a small concentration of chiral dopant to form a chiral nematic phase showed that $e = 2.7\ \mathrm{pCm^{-1}}$ at $T_r = 0.97$,[4] where $T_r = T(\mathrm{K})/T_{IN*}(\mathrm{K})$, ($T_{IN*}$ is the isotropic to chiral nematic transition temperature on cooling). To increase e/K and minimize dielectric coupling, bimesogenic compounds consisting of two mesogenic moieties that are attached by an alkyl chain have been developed in recent years.[5–7] These compounds exhibit larger e/K than conventional compounds in addition to a low $\Delta\varepsilon$. In addition, these bimesogenic structures, when combined with chiral dopants, exhibit blue phases that exist over an unusually wide temperature range.[8,9] There is current interest in the phase behaviour of such bimesogenic structures. For example, it was recently shown that 1″,7″-bis(4-cyanobiphenyl-4′-yl)heptane (CB7CB) has two liquid crystal mesophases on cooling, of which the higher temperature mesophase is nematic and the lower temperature mesophase is a new type of uniaxial nematic phase.[10] For bimesogens of similar generic structure, the lower temperature nematic mesophase has also been shown to exhibit linear switching in an electric field, despite consisting of non-chiral molecules.[11]

The flexoelectro-optic effect has been shown to operate in two different switching modes: the uniform lying helix (ULH) alignment (Fig. 1a) and the uniform-standing helix (USH) configuration (Fig. 1b). In ULH alignment the helical axis is in the plane of the device and an electric field is applied perpendicular to the substrates by means of planar electrodes on both substrates. The optic axis rotates in the plane of the device. The direction of rotation depends on the polarity of the applied field.[2] In the uniform-standing helix (USH) configuration, the helical axis is normal to the plane of the device and the LC is electrically addressed using in-plane electrodes.[12–14] Significant progress has been made in developing materials with higher e/K, however further development is still required in order to reduce the driving voltage to the level used in current active matrix display technologies, for example in-plane switching technology uses a peak-to-peak driving voltage of $\sim$8 V.[15] Such low driving voltages would allow use of current driver circuitry, overcoming one of the barriers to successful commercial exploitation of the technology.

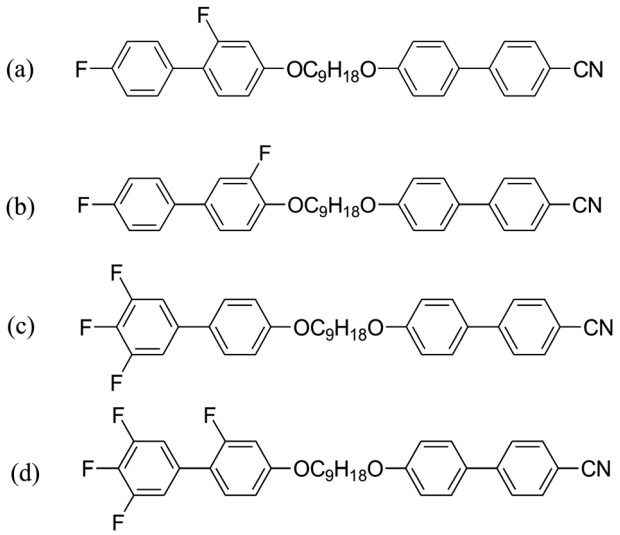

Fig. 1 Chemical structures of the ether-linked bimesogenic compounds used in this study. These included two di-fluorinated structures [(a) 1-(2′,4-Difuorobiphenyl-4′-yloxy)-9-(4-cyanobiphenyl-4′-yloxy)nonane (FFO9OCB) (b) 1-(3′,4-Difuorobiphenyl-4′-yloxy)-9-(4-cyanobiphenyl-4′-yloxy)nonane (FF′O9OCB)] one tri-fluorinated structure [(c) 1-(3,4,5-Trifuorobiphenyl-4′-yloxy)-9-(4-cyanobiphenyl-4′-yloxy)-nonane (F3O9OCB)] and one tetra-fluorinated structure [(d) 1-(2′,3,4,5-Tetrafluorobiphenyl-4′-yloxy)-9-(4-cyanobiphenyl-4′-yloxy)-nonane (F3FO9OCB)].

In this paper, we present data on the flexoelectro-optic and dielectric properties of a series of eight non-symmetric, fluorinated bimesogenic compounds, four of which have ether linkages and four of which have ester linkages. Bimesogenic structures show an "odd–even" effect in the flexoelastic ratio whereby the flexoelastic ratio is higher for bimesogens with an odd number of carbon atoms in the alkyl chain than those with an even-spaced chain. Therefore, a series of odd-spaced bimesogens was chosen for this study.[4,16] Furthermore, previous reports have indicated that the flexoelastic ratio is higher for ester-linked bimesogens compared with ether-linked bimesogens and that estimates suggest that this is due to larger values of the flexoelectric coefficient.[16–18] Consequently, the purpose of this study is to investigate the influence of the linking group in detail and the effect it has on both the flexoelectric and elastic coefficients of the bimesogens. We also examine the role that lateral and terminal substituted fluorine atoms have on the flexoelectro-optic properties. Specifically, it is shown that the magnitude of flexoelectro-optic switching in bimesogenic LCs can be increased by using highly fluorinated bimesogenic structures with ester linking groups.

2. Material synthesis and mixture preparation

A. Synthesis and characterisation

A series of bimesogenic structures with ether linkages were synthesized using the following procedure. 1,9-Dibromonoane (1 eq.) and 4′-hydroxy-4-biphenylcarbonitrile (1 eq.) were dissolved together in acetone before adding potassium carbonate. The resultant mixture was then refluxed for 2 days. On completion of this reaction, the filtrate was evaporated until dryness under

reduced pressure. The resultant crude material was then chromatographed (silica gel, dichloromethane (DCM) : Hexane (Hex), 3 : 1) and the first fraction was collected and evaporated to obtain 4′-(9-bromononyloxy)-4-biphenylcarbonitrile.

This bromoalkyl phenol ether and the second part of the appropriate phenol (1 eq.) were dissolved together in acetone before adding potassium carbonate. The resultant mixture was then refluxed for 4–7 days. On completion of this reaction, the filtrate was evaporated until dryness under reduced pressure. The resultant crude material was chromatographed (silica gel, DCM) and the major fraction was then collected and evaporated to obtain the desired product. The chemical structures of the ether-linked compounds are shown in Fig. 1. Confirmation of the structures was obtained by ^{1}H and ^{13}C NMR spectroscopy using a Bruker Avance III NMR spectrometer with a dual ^{13}C/^{1}H (126 MHz/500 MHz) cryprobe. The molecular mass was confirmed by mass spectrometry. The samples were run on a Thermo-Fisher Finnigan LTQ Orbitrap Mass Spectrometer by positive ion electrospray.

FFO9OCB. Yield 78%, ^{1}H NMR (500 MHz, $CDCl_3$) δ_H 7.66 (dd, J = 8.5, 2.0 Hz, 2H), 7.63 (dd, J = 8.5, 2.0 Hz, 2H), 7.57 (dd, J = 7.0, 2.0 Hz, 2H), 7.46 (ddd, J = 8.8, 5.3, 1.6 Hz, 2H), 7.29 (t, J = 8.8 Hz, 1H), 7.15–7.07 (m, 2H), 7.03–6.96 (m, 2H), 6.75 (dd, J = 8.5, 2.0 Hz, 1H), 6.70 (dd, J = 8.5, 2.0 Hz, 1H), 4.01 (t, J = 6.5 Hz, 2H), 3.98 (t, J = 6.5 Hz, 2H), 1.85–1.79 (m, 4H), 1.51–1.45 (m, 4H), and 1.42–1.37 (m, 6H). ^{13}C NMR (126 MHz, $CDCl_3$) δ_c 162.22 (d, J = 241.8 Hz), 160.60 (d, J = 241.8 Hz), 159.90 (d, J = 3.7 Hz), 159.29, 145.40, 132.69, 131.90 (d, J = 3.7 Hz), 131.40, 130.93 (d, J = 3.7 Hz), 130.48 (dd, J = 8.3, 3.7 Hz), 128.45, 127.20, 120.31 (d, J = 13.8 Hz), 119.25, 115.45 (d, J = 13.8 Hz), 115.21, 111.00 (d, J = 3.7 Hz), 110.17, 102.64 (d, J = 13.8 Hz) 68.27, 29.59, 25.43, 29.40, 29.35, 29.24, 26.16, and 26.12; ESI-HRMS obsd 526.2532 ($[M + H]^+$), calcd 526.2552 ($[M + H]^+$), 525.6281 ($[M]^+$), ($M = C_{34}H_{33}F_2NO_2$).

FF′O9OCB. Yield 65%, ^{1}H NMR (500 MHz, $CDCl_3$) δ_H 7.68 (d, J = 7.8 Hz, 2H), 7.63 (d, J = 8.2 Hz, 2H), 7.56–7.50 (m, 2H), 7.47 (dd, J = 8.4, 4.6 Hz, 2H), 7.27 (d, J = 8.4 Hz, 1H), 7.22 (d, J = 8.4 Hz, 1H), 7.14–7.07 (m, 2H), 7.05–6.96 (m, 3H), 4.07 (t, J = 6.5 Hz, 2H), 4.02 (t, J = 6.5 Hz, 2H), 1.88–1.79 (m, 4H), 1.50–1.48 (m, 4H), and 1.41–1.39 (m, 6H). ^{13}C NMR (126 MHz, $CDCl_3$) δ_c 162.44 (d, J = 246.5 Hz), 159.91, 152.93 (d, J = 246.5 Hz), 146.63 (d, J = 13.4 Hz), 145.38, 136.01, 133.47 (d, J = 8.1 Hz), 132.67, 131.36, 128.43, 128.33 (d, J = 8.1 Hz), 127.17, 122.58 (d, J = 3.4 Hz), 119.26, 115.81 (d, J = 13.4 Hz), 115.20, 114.85 (d, J = 13.4 Hz), 110.14, 69.66, 68.26, 29.56, 29.39, 29.33, 26.13, and 26.04; ESI-HRMS obsd 526.2541 ($[M + H]^+$), calcd 526.2552 ($[M + H]^+$), 525.6281 ($[M]^+$), ($M = C_{34}H_{33}F_2NO_2$).

F3O9OCB. Yield 62%, 1H NMR (500 MHz, $CDCl_3$) δ_H 7.69 (d, J = 7.7 Hz, 2H), 7.64 (d, J = 7.7 Hz, 2H), 7.52 (d, J = 7.7 Hz, 2H), 7.41 (d, J = 7.7 Hz, 2H), 7.14–7.11 (m, 2H), 6.99(d, J = 7.7 Hz, 2H), 6.96 (d, J = 7.7 Hz, 2H), 4.03–3.98 (m, 4H), 1.84–1.79 (m, 4H), 1.50–1.39 (m, 4H), and 1.40 (m, 6H). ^{13}C NMR (126 MHz, $CDCl_3$) δ_c 159.92, 159.60, 151.52 (dd, J = 249.5, 15.9 Hz), 145.40, 138.85 (ddd, J = 249.5, 15.9, 5.0 Hz), 137.25–137.08 (m), 132.70, 131.42, 130.57, 128.46, 128.03, 127.20, 119.25, 115.21, 115.14, 110.54 (dd, J = 15.9, 5.0 Hz), 110.19, 68.28, 29.61, 29.44, 29.36, and 26.16; ESI-HRMS obsd 544.2435 ($[M + H]^+$), calcd 544.2458 ($[M + H]^+$), 543.6186 ($[M]^+$), ($M = C_{34}H_{32}F_3NO_2$).

F3FO9OCB. Yield 60%,^{1}H NMR (500 MHz, $CDCl_3$) δ_H 7.69 (d, J = 8.1 Hz, 2H), 7.64 (d, J = 8.1 Hz, 2H), 7.53 (d, J = 8.1 Hz, 2H), 7.30–7.22 (m, 1H), 7.13 (t, J = 8.1 Hz, 2H), 7.05–6.96 (m, 2H), 6.80–6.73 (m, 1H), 6.71–6.68 (m, 1H), 4.03–3.96 (m, 4H), 1.84–1.79 (m, 4H), 1.51–1.46 (m, 4H), and 1.40–1.39 (m, 6H). ^{13}C NMR (126 MHz, $CDCl_3$) δ_c 160.25 (d, J = 251.6 Hz), 160.74 (d, J = 15.3 Hz), 159.91, 151.20 (ddd, J = 251.6, 15.3, 4.7 Hz), 145.39, 139.05 (dt, J = 251.6, 15.3 Hz), 132.69, 131.93–131.82 (m), 131.41, 130.60 (d, J = 4.7 Hz), 128.45, 127.19, 119.24, 118.25 (d, J = 15.3 Hz), 115.20, 112.86 (dt, J = 15.3, 4.7 Hz), 111.32, 111.30, 110.18,110.18, 102.78 (d, J = 15.3 Hz), 68.64, 68.26, 29.59, 29.43, 29.39, 29.35, 29.28, 29.18, 26.16, and 26.10. ESI-HRMS obsd 562.2344 ($[M + H]^+$), calcd 562.2364 ($[M + H]^+$), 561.6091 ($[M]^+$), ($M = C_{34}H_{31}F_4NO_2$).

The ester linkage molecules were synthesized using the following procedure. Undecandioic acid, *N*,*N*′-dicyclohexylcarbodiimide (DCC), and 4-dimethylaminopyridine (DMAP), in equimolar quantities, were dissolved in chilled DCM. The reaction mixture was then stirred at ~5 °C for 20 minutes while adding one part of the appropriate phenol (1 eq.). The resultant mixture was brought to room temperature and stirred for 24 hours in a sealed container. This was followed by the addition of a mixture of 4′-hydroxy-4-biphenylcarbonitrile and DCC (equimolar quantities) and stirred at room temperature for next three days. Once the reaction was finished, the filtrate was evaporated to dryness under reduced pressure. The resultant crude material was chromatographed (silica gel, DCM) and the second major fraction was collected and evaporated to obtain the desired product. The chemical structures of the ester linked compounds are shown in Fig. 2.

FFE9ECB. Yield 52%, ^{1}H NMR (500 MHz, $CDCl_3$) δ_H 7.71 (dd, J = 8.8, 2.1 Hz, 2H), 7.65 (dd, J = 8.8, 2.1 Hz, 2H), 7.58 (dd, J = 7.0, 2.0 Hz, 2H), 7.48 (ddd, J = 8.8, 5.3, 1.6 Hz, 2H), 7.39 (t, J = 8.7 Hz, 1H), 7.21 (m, 2H), 7.16–7.09 (m, 2H), 7.00–6.92 (m, 2H), 2.59 (t, J = 7.1 Hz, 4H), 1.74–1.81 (m, 4H), and 1.49–1.35 (m, 10H). ^{13}C NMR (126 MHz, $CDCl_3$) δ_c 172.32, 172.06, 162.60 (d, J = 247.4 Hz), 159.53 (d, J = 247.4 Hz), 151.33, 150.80 (d, J = 8.1 Hz), 144.91, 136.88, 132.77, 131.19 (d, J = 3.6 Hz), 130.93 (d, J = 3.6 Hz), 130.74 (dd, J = 8.1, 3.6 Hz), 128.45, 127.79, 125.84 (d, J = 13.6 Hz), 122.45, 118.98, 117.87 (d, J = 3.6 Hz), 115.62 (d, J = 13.6 Hz), 111.15, 110.36 (d, J = 13.6 Hz). 34.51, 34.44, 29.36, 29.30, 29.19, 29.17, 25.02, and 24.97. ESI-HRMS obsd 582.2424 ($[M + H]^+$), calcd 582.2450 ($[M + H]^+$), 581.6483 ($[M]^+$), ($M = C_{36}H_{33}F_2NO_4$).

FF′E9ECB. Yield 32.5%, ^{1}H NMR (500 MHz, $CDCl_3$) δ_H 7.71 (d, J = 8.2 Hz, 2H), 7.65 (d, J = 8.2 Hz, 2H), 7.58 (dd, J = 8.2, 1.8 Hz, 2H), 7.52–7.46 (m, 2H), 7.28 (d, J = 8.2 Hz, 1H), 7.22 (d, J = 8.2 Hz, 1H), 7.14–7.07 (m, 2H), 7.08–6.99 (m, 3H), 2.70–2.51 (m, 4H), 1.86–1.68 (m, 4H, CH_2), and 1.53–1.30 (m, 10H, CH_2). ^{13}C NMR (126 MHz, $CDCl_3$) δ_c

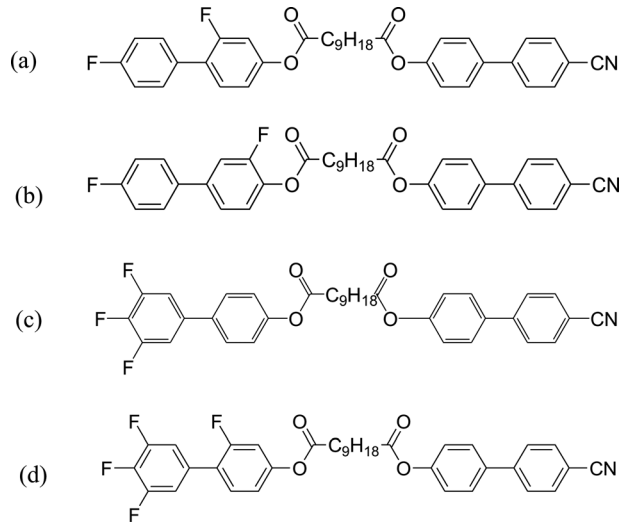

Fig. 2 Chemical structures of the ester-linked bimesogenic compounds used in this study. These included two di-fluorinated structures [(a) 1-(2′,4-Difuorobiphenyl-4′-yl)-9-(4-cyanobiphenyl-4′-yl) undecandioate (FFE9ECB) (b) 1-(3′,4-Difuorobiphenyl-4′-yl)-9-(4-cyanobiphenyl-4′-yl) undecandioate (FF′E9ECB)] one tri-fluorinated structure [(c) 1-(3,4,5-Trifuorobiphenyl-4′-yl)-9-(4-cyanobiphenyl-4′-yl) undecandioate (F3E9ECB)] and one tetra-fluorinated structure [(d) 1-(2′,3,4,5-Tetrafuorobiphenyl-4′-yl)-9-(4-cynobiphenyl-4′-yl) undecandioate (F3FE9ECB)].

172.33, 171.4, 162.85 (d, J = 249.1 Hz), 154.29 (d, J = 249.1 Hz), 151.21, 144.78, 139.64 (d, J = 8.1 Hz), 137.36 (d, J = 13.1 Hz), 136.74, 135.46, 132.63, 128.66 (d, J = 8.1 Hz), 128.31, 127.66, 124.98, 124.00, 122.87 (d, J = 3.3 Hz), 122.33, 120.33 (d, J = 13.1 Hz), 118.86, 118.77 (d, J = 8.1 Hz), 115.84 (d, J = 13.1 Hz), 115.23 (d, J = 13.1 Hz), 111.01, 34.51, 34.04, 33.93, 29.34, 29.26, 29.17, 29.08, 29.05, and 24.94. ESI-HRMS obsd 604.2244 ($[M + Na]^+$), calcd 604.2270 ($[M + Na]^+$), 581.6483 ($[M]^+$), ($M = C_{36}H_{33}F_2NO_4$).

F3E9ECB. Yield 33%, ^{1}H NMR (500 MHz, $CDCl_3$) δ_H 7.72 (d, J = 8.0 Hz, 2H), 7.65 (d, J = 8.0 Hz, 2H), 7.59 (d, J = 8.0 Hz, 2H), 7.52–7.46 (m, 2H, ArH), 7.21–7.14 (m, 6H), 2.61–2.57 (m, 4H), 1.81–1.75 (m, 4H), and 1.48–1.36 (m, 10H). ^{13}C NMR (126 MHz, $CDCl_3$) δ_c 172.34, 151.42 (ddd, J = 253.2, 15.1, 4.7 Hz), 151.33, 151.08, 144.91, 140.58, 139.42 (dt, J = 253.2, 15.1 Hz), 136.90, 136.63–136.61 (m), 135.95, 132.98, 128.46, 128.08, 127.80, 122.44 (d, J = 4.7 Hz), 118.98, 111.75–110.81 (m), 34.51, 29.37, 29.31, 29.20, and 25.02; ESI-HRMS obsd 622.2161 ($[M + Na]^+$), calcd 622.2176 ($[M + Na]^+$), 599.6388 ($[M]^+$), ($M = C_{36}H_{32}F_3NO_4$).

F3FE9ECB. Yield 30%, ^{1}H NMR (500 MHz, $CDCl_3$) δ_H 7.72 (d, J = 8.0 Hz, 2H), 7.65 (d, J = 8.0 Hz, 2H), 7.59 (d, J = 8.0 Hz, 2H), 7.37 (t, J = 8.0 Hz, 1H), 7.20 (d, J = 8.0 Hz, 2H), 7.16–7.13 (m, 2H), 7.00–6.97 (m, 2H), 2.61–2.57 (m, 4H), 1.80–1.75 (m, 4H), and 1.48–1.35 (m, 10H). ^{13}C NMR (126 MHz, $CDCl_3$) δ_c 172.34, 171.90, 159.46 (d, J = 251.0 Hz), 152.32–151.61 (m), 151.33, 150.34–150.23 (m), 144.91, 139.60 (dt, J = 251.0, 14.4 Hz), 136.91, 132.78, 131.05, 130.65, 130.62, 128.46, 127.81, 123.82 (d, J = 14.4 Hz), 122.46, 118.98, 118.24 (d, J = 4.4 Hz), 113.38–113.18 (m), 111.18, 110.63 (d, J = 14.4 Hz), 34.52, 34.43, 29.36, 29.30, 29.20, 29.16, 25.02, and 24.93; ESI-HRMS obsd 640.2050 ($[M + Na]^+$), calcd 640.2081 ($[M + Na]^+$), 617.6293 ($[M]^+$), ($M = C_{36}H_{31}F_4NO_4$).

B. Chiral nematic mixtures

For the flexoelectro-optic measurements, mixtures were prepared in which a chiral nematic phase was induced by the high twisting power, sorbitol-based chiral dopant BDH1281[19] (Merck KGaA) at a concentration of approximately 3.5 wt%. Each sample was heated into the isotropic phase and then left at 130 °C for one hour, before being held in the chiral nematic phase for >24 hours to allow for thermal diffusion. The mixtures were capillary filled into cells whose inner substrates were coated with anti-parallel rubbed polyimide alignment layers. Indium tin oxide electrodes enabled the application of an electric field normal to the substrates. The cell gaps, defined by spacer beads within the glue, were measured from optical interference measurements. For all compounds, the pitch of the doped compounds increases, as the reduced temperature decreases.

3. Experimental methods

The mesomorphic behaviour of the compounds was determined using a polarizing optical microscope (BH2, Olympus) that was fitted with a hot-stage (THMS 600, Linkam) and a temperature controller (TP94, Linkam) and confirmed with data obtained using a differential scanning calorimeter (DSC) (Mettler-Toledo DSC823^e). DSC transition temperatures were determined both on heating and cooling at a rate of 5 °C min^{-1}.

A single-cell method[20–22] was used to measure the capacitance and to obtain both dielectric permittivities. Experiments were carried out using 20 μm anti-parallel, planar aligned cells and a precision component analyzer (6440A, WK electronics). The frequency was 10 kHz. The two elastic coefficients were both determined from the capacitance measurements using a numerical fitting procedure based on the Oseen–Frank free energy.

Measurements of the tilt angle of the optic axis were carried out by positioning the sample on the hot stage of a polarizing microscope with a rotatable stage and an objective with a magnification of 20×. A bipolar electric field (100 Hz square wave) was applied across the sample. The ULH texture had to be induced to satisfy the condition of an electric field that was orthogonal to the helix axis. This was achieved by cooling the sample from the isotropic phase in the presence of the field. If necessary, mechanical pressure was applied to the cell, by prodding it with tweezers to help form the ULH. The optical response was measured using a fast response time photodiode (PDA55, Thorlabs) and recorded by a digitizing oscilloscope (HP54503A, Hewlett-Packard). In order to ensure maximum contrast in the photodetector response, the unperturbed optic axis of the chiral nematic was aligned at 22.5° to the transmission axis of one of the polarizers. The angle between the two switched states is given by 2ϕ. The response time was measured as the average of the time for the intensity to increase from 10% to 90% or *vice versa* for change in the polarity of the applied field. Finally, in order to extract e/K and γ/K, the pitch of each chiral nematic sample was measured using the Cano Wedge method.[23–25]

4. Results and discussion

A. Mesophase characterization

The transition temperatures and enthalpy changes of transitions on heating, taken from DSC measurements are shown in Table 1. For most compounds, the width of the nematic phase was >20 °C both on heating and cooling, with the exception of F3E9ECB which is monotropic. From DSC measurements, the nematic phase was found to supercool over a 20.5 °C temperature range. However, if left for ~1 hour, the sample would crystallize at considerably higher temperatures. In general, the nematic phase of the non-symmetric ester-linked compounds investigated in this study were thermodynamically stable over a much wider temperature range than that observed for similar symmetric bimesogens previously characterized, which were found to be monotropic.[17] Three of the compounds appear to show an additional LC phase below the nematic phase in which measurements were carried out. Further work is being carried out to establish the nature of this phase.

For both the ether-linked and ester-linked series of compounds, the nematic to isotropic transition temperature on heating T_{NI} was substantially reduced by the addition of fluoro substituents. To illustrate this point T_{NI} ranged from 112.7 °C for FFE9ECB to 79.6 °C for F3FE9ECB. This reduction in transition temperature is commonly observed for LCs with lateral fluoro substituents. Whilst the fluoro substituents are small enough for a relatively wide LC phase range to be preserved, lateral fluoro substituents tend to disrupt the intermolecular forces and molecular packing.[26] There is no consistent change in transition temperatures on changing the linking group from an ether to an ester linkage. For all compounds, the melting enthalpy is about an order of magnitude larger than the enthalpy associated with the transition into the isotropic, indicating that the structural change from the crystalline phase into the lowest order mesophase is considerably larger than for the nematic to isotropic transition.

B. Dielectric properties

As stated in the introduction, $\Delta\varepsilon$ plays an important role in determining the critical unwinding field amplitude, at which point the helical structure is removed and flexoelectro-optic switching can no longer occur. Fig. 3 shows $\Delta\varepsilon$ as a function of T_r† for all eight compounds. The general trend for both types of linkage is that $\Delta\varepsilon$ decreases with an increase in the number of fluoro substituents. For the ether-linked bimesogens (Fig. 3a), $\Delta\varepsilon$ is highest for the bimesogen FF′O9OCB, taking a value of $\Delta\varepsilon = 4.8 \pm 0.2$ at $T_r = 0.969 \pm 0.005$. Changing the position of the lateral fluoro substituent, however, substantially reduces $\Delta\varepsilon$ (for example, for FFO9OCB, $\Delta\varepsilon = 3.4 \pm 0.2$ at $T_r = 0.969 \pm 0.005$). Moreover, the value of $\Delta\varepsilon$ is reduced further still on the addition of more terminal fluoro substituents. This can be seen for F3O9OCB whereby $\Delta\varepsilon = 2.9 \pm 0.2$ at $T_r = 0.967 \pm 0.006$ and for F3FO9OCB, $\Delta\varepsilon = 2.7 \pm 0.2$ at $T_r = 0.971 \pm 0.006$.

Table 1 Transition temperatures (°C) and enthalpies (mJ g^{-1}) on heating for the non-symmetric bimesogen compounds. Enthalpy values are shown in parentheses and values for monotropic compounds are shown on cooling, indicated by an asterix. A dagger is used to indicate compounds that appear to have an additional LC phase on heating

Compound	Cr		N		Iso
FFO9OCB	•	42.3 (33.6)	•	108 (3.4)	•
FF′O9OCB	•	73.1 (128.3)	•	103.1 (5.5)	•
F3O9OCB†	•	80.8 (1.6)	•	90.1 (0.3)	•
F3FO9OCB	•	61.9 (34.8)	•	73.9 (1.4)	•
FFE9ECB	•	86.6 (57.4)	•	112.7 (4.5)	•
FF′E9ECB†	•	76.3 (26.2)	•	96.0 (2.4)	•
F3E9ECB*	•	67.2 (87.6)	•	87.7 (3.0)	•
F3FE9ECB†	•	66.8 (8.9)	•	79.6 (7.5)	•

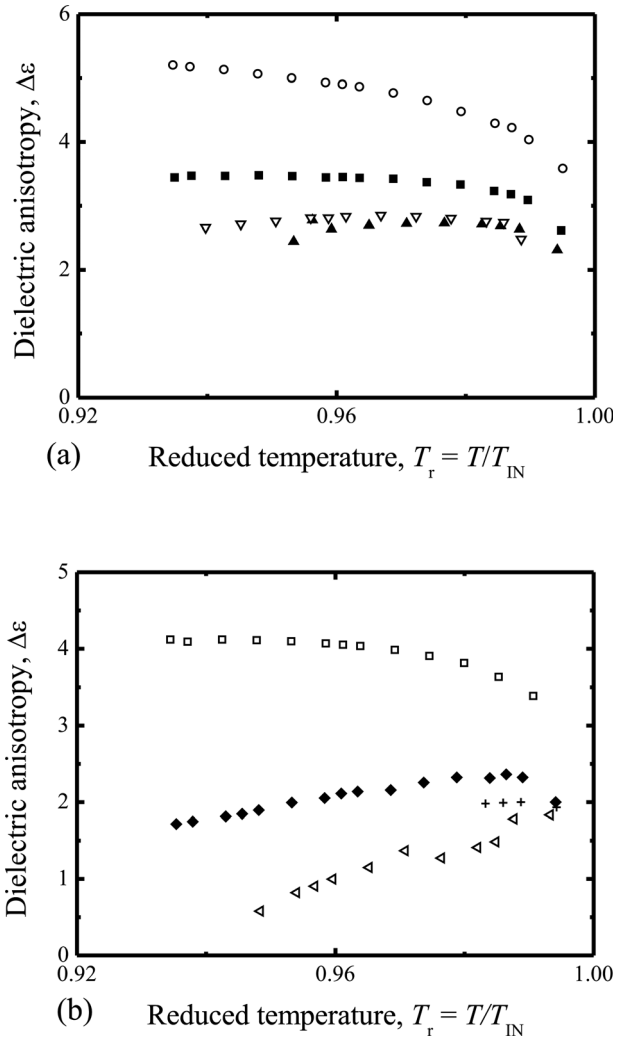

Fig. 3 (a) Dielectric anisotropy $\Delta\varepsilon$ as a function of reduced temperature for the series of ether-linked bimesogenic compounds: FFO9OCB (■), FF′O9OCB (○), F3FO9OCB (▲), F3O9OCB (▽). (b) Dielectric anisotropy as a function of reduced temperature for the series of ester-linked bimesogenic compounds: FFE9ECB (◆), FF′E9ECB (□), F3FE9ECB (◁), F3E9ECB (+).

† For measurements of dielectric permittivities and elastic coefficients $T_r = T(K)/T_{IN}(K)$. For measurements taken with a chiral dopant added to the compound, for example flexoelastic ratios and viscoelastic ratios, $T_r = T(K)/T_{IN*}(K)$.

For the ester-linked bimesogens, altering the position of the lateral fluoro substituent also appears to change the dielectric anisotropy quite significantly (Fig. 3b); for example, for FF′E9ECB, $\Delta\varepsilon = 4.0 \pm 0.2$ at $T_r = 0.969 \pm 0.006$, which is larger than that recorded for the compound FFE9ECB whereby $\Delta\varepsilon = 2.2 \pm 0.2$ at $T_r = 0.969 \pm 0.005$. Furthermore, $\Delta\varepsilon$ is decreased further as the number of fluoro substituents is increased. This is evident for the compound F3FE9ECB, $\Delta\varepsilon = 1.4 \pm 0.2$ at $T_r = 0.971 \pm 0.006$. For comparison, the nearest available data for F3E9ECB was $\Delta\varepsilon = 2.0 \pm 0.2$ at a reduced temperature of $T_r = 0.983 \pm 0.006$, which also fits within this trend. The values of $\Delta\varepsilon$ of the ester-linked compounds are consistently lower than those of the equivalent ether-linked compounds (*cf.*, Fig. 3a).

C. Flexoelastic properties

To maximize the tilt angle, a large e/K is required as emphasized in eqn (2). The e/K ratios of all compounds are shown as a function of reduced temperature in Fig. 4. Irrespective of the type of linkage, altering the number of fluoro substituents appears to cause notable changes to e/K. For both analogues, e/K is lowest for the compounds where the terminal phenyl ring is mono-substituted. Experimental values of e/K for the mono-substituted ether-linked bimesogens, FFO9OCB and FF′O9OCB were $e/K = 1.06 \pm 0.05$ CN^{-1} m^{-1} at $T_r = 0.967 \pm 0.006$ and $e/K = 0.89 \pm 0.04$ CN^{-1} m^{-1} at $T_r = 0.965 \pm 0.005$, respectively. The magnitude of e/K can be increased by having a tri-fluoro substituted terminal phenyl group as shown in the data for F3O9OCB ($e/K = 1.36 \pm 0.07$ CN^{-1} m^{-1} at $T_r = 0.974 \pm 0.005$). For the bimesogen with both a tri-fluoro substituted terminal phenyl group and a lateral fluoro on the second phenyl ring, e/K is further increased to 1.65 ± 0.08 CN^{-1} m^{-1} at $T_r = 0.972 \pm 0.006$. The largest change in e/K observed is on replacing an ether linkage with an ester linkage, Fig. 4b. Of the eight compounds, the largest value of e/K recorded was for F3FE9ECB, for which $e/K = 2.64 \pm 0.13$ CN^{-1} m^{-1} at $T_r = 0.969 \pm 0.006$. This value is almost a factor of 6 times greater than that recorded for a typical monomesogen such as 7OCB ($e/K = 0.46$ at $T_r = 0.972$), which was measured using the same experimental apparatus. It is also significantly higher than the highest previously recorded value for a single bimesogenic compound of $e/K = 1.6 \pm 0.08$ CN^{-1} m^{-1} at $T_r = 0.840 \pm 0.005$ for NSO9OFF (1-(2′,4-difluorobiphenyl-4′-yloxy)-9-(4-nitrostilben-4′-yloxy)-nonane).[16]

To determine the relative contributions to e/K, values of e have been calculated using experimental values of K and the results are plotted as a function of reduced temperature for both the ether-linked and ester-linked structures in Fig. 5. The most striking feature is that e is considerably higher for the ester-linked bimesogenic compounds compared with the ether-linked compounds, in accordance with previous findings based upon an approximation using only K_1.[16,18] As an example, at $T_r = 0.969 \pm 0.006$, $e = 12.6 \pm 0.6$ pCm^{-1} for F3FE9ECB compared with $e = 8.0 \pm 0.4$ pCm^{-1} for F3FO9OCB at $T_r = 0.972 \pm 0.006$. It is clear that the ester-linked compound has a larger flexoelectric coefficient. One explanation might be that, if taken in the context of dipolar theory,[25] the increase in e for the ester-linked compounds could be the result of an increase in the transverse dipole moment. This in turn results in an increase in the bend flexoelectric coefficient. Values of e for both the ether and ester-linked bimesogens are significantly greater than those reported recently for 7OCB ($e = 2.7$ pCm^{-1} at $T_r = 0.97$) using the same experimental procedure.[4]

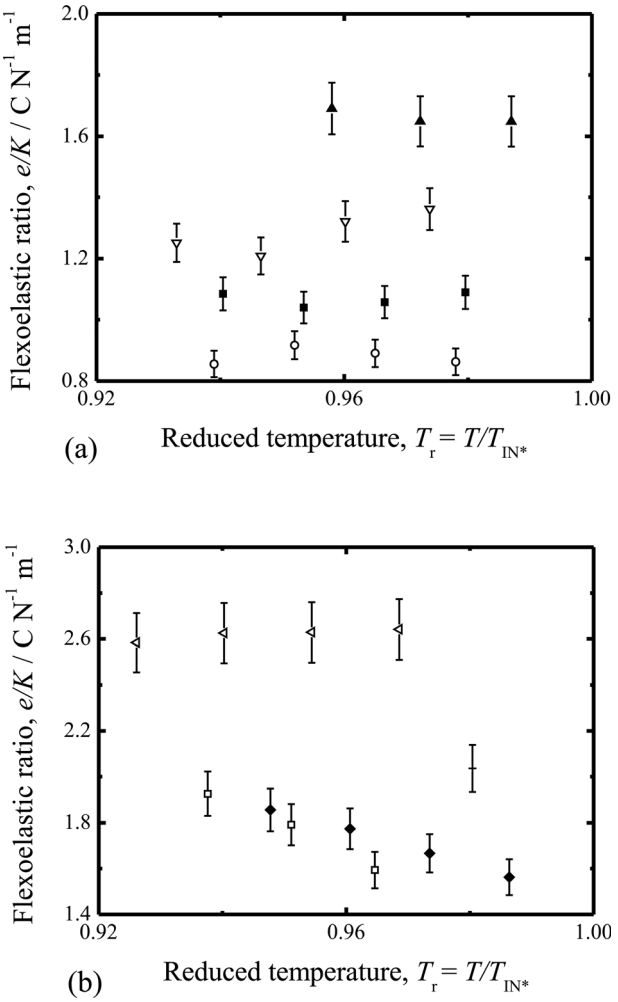

Fig. 4 (a) Flexoelastic ratio e/K as a function of reduced temperature for the series of ether-linked bimesogenic compounds: FFO9OCB (■), FF′O9OCB (○), F3FO9OCB (▲), F3O9OCB (▽). (b) Flexoelastic ratio as a function of reduced temperature for the series of ester-linked bimesogenic compounds: FFE9ECB (◆), FF′E9ECB (□), F3FE9ECB (◁), F3E9ECB (+).

For the ether-linked compounds, the value of e also seems to vary with the number and position of fluoro substituents (Fig. 5a). Compounds with a greater number of fluoro substituents appear to have higher flexoelectric coefficients. As an example, for F3O9OCB, $e = 8.0 \pm 0.4$ pCm^{-1} at a reduced temperature of $T_r = 0.972 \pm 0.006$, compared to FF′O9OCB, $e = 5.9 \pm 0.3$ pCm^{-1} at a reduced temperature of $T_r = 0.973 \pm 0.005$. The value of e for the ester-linked compounds, however, does not appear to change significantly with the number or position of the fluoro substituents.

Plots of K are presented as a function of reduced temperature in Fig. 6 for completeness where it can be seen that there is no clear change in K on changing the linking group from ether

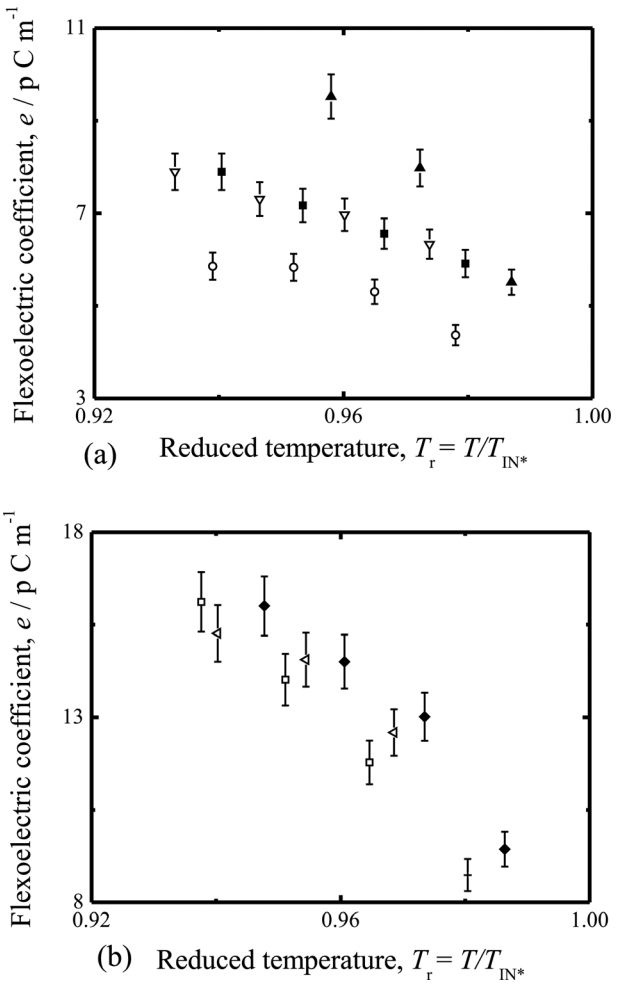

Fig. 5 (a) Effective flexoelectric coefficient e as a function of reduced temperature for the series of ether-linked bimesogenic compounds: FFO9OCB (■), FF′O9OCB (○), F3FO9OCB (▲), F3O9OCB (▽). (b) Effective flexoelectric coefficient as a function of reduced temperature for the series of ester-linked bimesogenic compounds: FFE9ECB (◆), FF′E9ECB (□), F3FE9ECB (◁), F3E9ECB (+).

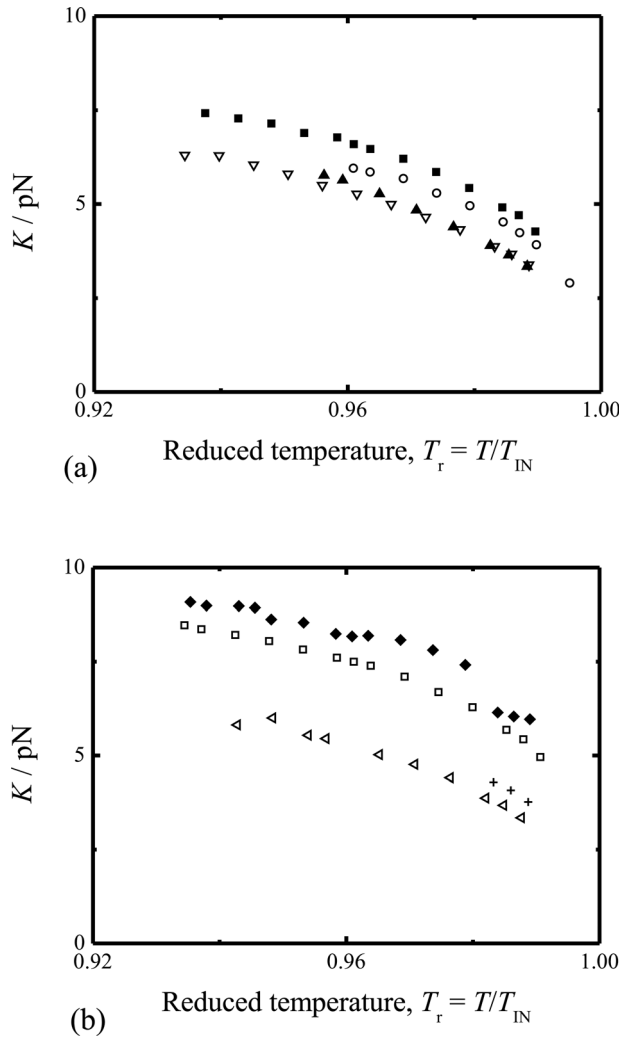

Fig. 6 Effective elastic coefficients K as a function of reduced temperature for the series of ether-linked bimesogenic compounds (a): FFO9OCB (■), FF′O9OCB (○), F3FO9OCB (▲), F3O9OCB (▽). (b) Effective elastic coefficients as a function of reduced temperature for the series of ester-linked bimesogenic compounds: FFE9ECB (◆), FF′E9ECB (□), F3FE9ECB (◁), F3E9ECB (+).

to ester. The magnitude of K does, however, decrease with the addition of more fluorine atoms: this is observed for both the ether and ester-linked compounds. For example, K = 7.8 pN for FFE9ECB at T_r = 0.973 ± 0.005 by comparison with K = 4.8 pN for F3FE9ECB at T_r = 0.969 ± 0.006. These results indicate that, for a given linking group, the increase in e/K with a larger number of fluoro substituents is in the most part due to a decrease in K. The increase in e/K by replacing ether-linkages with ester-linkages is, on the other hand, the result of a dramatic increase in e.

D. Viscoelastic ratios

The final important parameter is γ/K as this governs the response time (eqn (3)). A low γ/K is essential for fast switching of the optic axis. Values of γ/K have been extracted from the measurements of the response time and the pitch, and are shown as a function of reduced temperature for both the ether-linked and ester-linked compounds in Fig. 7. The results show that the position and number of fluoro substituents causes substantial changes in γ/K for both sets of compounds. Increasing the number of fluorine atoms appears to significantly increase γ/K. For example, at T_r = 0.972 ± 0.006 the viscoelastic ratio of F3FO9OCB is γ/K = 1.8 ± 0.1 × 10^{11} $PaN^{-1}s$ whereas at T_r = 0.967 ± 0.006, the γ/K ratio of FFO9OCB is found to be an order of magnitude lower, γ/K = 3.1 ± 0.2 × 10^{10} $PaN^{-1}s$. Furthermore, the values of γ/K of the ether-linked compounds are higher than those of the ester-linked compounds. The values of γ are presented in Fig. 8 demonstrating that γ increases with the number of fluorine atoms but are lower for the ester-linked compounds in comparison with their ether-linked counterparts.

5. Conclusions

In this paper, we have studied the flexoelectric, dielectric, and elastic properties of eight non-symmetric bimesogens. Results demonstrate that the flexoelastic ratio e/K and the flexoelectric

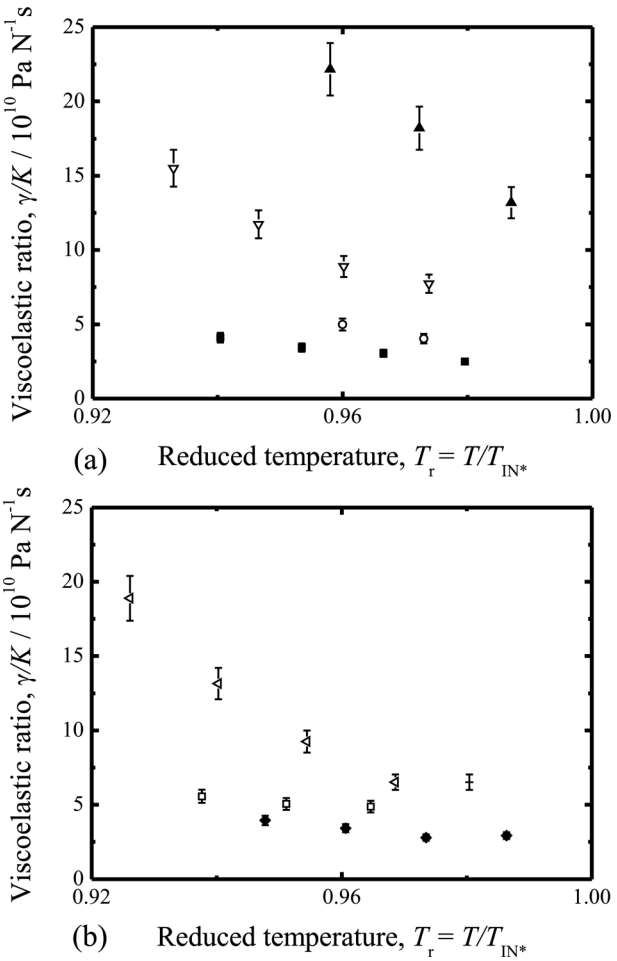

Fig. 7 (a) Viscoelastic ratio γ/K as a function of reduced temperature for the series of ether-linked bimesogenic compounds: FFO9OCB (■), FF′O9OCB (○), F3FO9OCB (▲), F3O9OCB (▽). (b) Viscoelastic ratio as a function of reduced temperature for the series of ester-linked bimesogenic compounds: FFE9ECB (◆), FF′E9ECB (□), F3FE9ECB (◁), F3E9ECB (+).

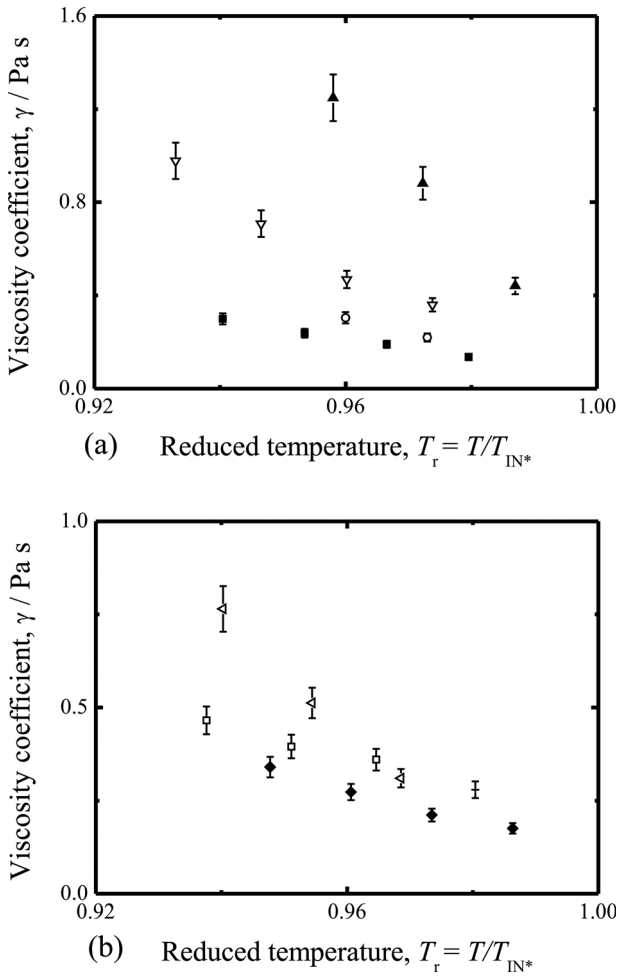

Fig. 8 (a) Viscosity coefficient γ as a function of reduced temperature for the series of ether-linked bimesogenic compounds: FFO9OCB (■), FF′O9OCB (○), F3FO9OCB (▲), F3O9OCB (▽). (b) Viscosity coefficient as a function of reduced temperature for the series of ester-linked bimesogenic compounds: FFE9ECB (◆), FF′E9ECB (□), F3FE9ECB (◁), F3E9ECB (+).

coefficients e of bimesogenic structures can be substantially enhanced using highly fluorinated mesogenic units with ester-linkages. By increasing the number of fluoro substituents and changing the linkage from ether to ester units, it is shown that e/K increases from 0.9 CN^{-1} m^{-1} to 2.6 CN^{-1} m^{-1}. These values are much higher than that reported for a conventional monomesogenic compound such as 7OCB whereby e/K = 0.46 at T_r = 0.972 and previously reported bimesogenic compounds.[5,16] Furthermore, e is found to be as large as 16 pCm^{-1} for the ester-linked compounds compared with e = 2.7 pCm^{-1} for 7OCB. The highly-fluorinated, ester linked structures also exhibit lower dielectric anisotropies (*e.g.* $\Delta\varepsilon$ = 1.4) and thus the critical field for helix-unwinding is higher for these structures ensuring that flexoelectric coupling will dominate up to relatively high electric field amplitudes. Adding fluoro substituents to the bimesogenic structures also reduces the clearing point but does, however, adversely affect their response time, since the more heavily fluorinated structures have higher viscoelastic ratios. Nevertheless, ester-linked compounds have lower viscoelastic ratios than the ether-linked compounds ensuring that fast response times are obtainable. In the context of devices, for materials of the same pitch, the ester-linked compounds will therefore show faster response times than the ether-linked compounds. Overall, due to their high flexoelastic ratios, low dielectric anisotropies and relatively low viscoelastic ratios, highly fluorinated, bimesogens are promising materials for use in flexoelectro-optic devices.

Acknowledgements

The authors gratefully acknowledge the Engineering and Physical Sciences Research Council (UK) and LG Display for financial support. One of the authors (K.A.) also acknowledges Merck UK for a CASE studentship and one of the authors (S.M.M) gratefully acknowledges The Royal Society for financial support. The authors would also like to thank Shabeena Nosheen for her contribution to the synthesis of the compounds investigated; Asha Boodhun for the mass spectrometry data and Duncan Howe, Dr Peter Grice and Andrew Mason for the NMR measurements.

References

1 R. B. Meyer, *Phys. Rev. Lett.*, 1969, **22**, 918.
2 J. S. Patel and R. B. Meyer, *Phys. Rev. Lett.*, 1987, **58**, 1538.
3 J. S. Patel and S. D. Lee, *J. Appl. Phys.*, 1989, **66**, 1879.
4 K. L. Atkinson, S. M. Morris, F. Castles, M. M. Qasim, D. J. Gardiner and H. J. Coles, *Phys. Rev. E: Stat., Nonlinear, Soft Matter Phys.*, 2012, **85**, 012701.
5 H. J. Coles, B. Musgrave, M. J. Coles and J. Willmott, *J. Mater. Chem.*, 2001, **11**, 2709.
6 C. Noot, M. J. Coles, B. Musgrave, S. P. Perkins and H. J. Coles, *Mol. Cryst. Liq. Cryst.*, 2001, **366**, 725.
7 B. Musgrave, P. Lehmann and H. J. Coles, *Liq. Cryst.*, 1999, **26**, 1235.
8 F. Castles, S. M. Morris, E. M. Terentjev and H. J. Coles, *Phys. Rev. Lett.*, 2010, **104**, 157801.
9 H. J. Coles and M. N. Pivnenko, *Nature*, 2005, **436**, 997.
10 M. Cestari, S. Diez-Berart, D. A. Dunmur, A. Ferrarini, M. R. de la Fuente, D. J. B. Jackson, D. O. Lopez, G. R. Luckhurst, M. A. Perez-Jubindo, R. M. Richardson, J. Salud, B. A. Timimi and H. Zimmermann, *Phys. Rev. E: Stat., Nonlinear, Soft Matter Phys.*, 2011, **84**, 031704.
11 V. P. Panov, R. Balachandran, M. Nagaraj, J. K. Vij, M. G. Tamba, A. Kohlmeier and G. H. Mehl, *Appl. Phys. Lett.*, 2011, **99**, 261903.
12 B. J. Broughton, M. J. Clarke, A. E. Blatch and H. J. Coles, *J. Appl. Phys.*, 2005, **98**, 034109.
13 F. Castles, S. M. Morris, D. J. Gardiner, Q. M. Malik and H. J. Coles, *J. Soc. Inf. Disp.*, 2010, **18**, 128.
14 F. Castles, S. M. Morris and H. J. Coles, *Phys. Rev. E: Stat., Nonlinear, Soft Matter Phys.*, 2009, **80**, 031709.
15 M. Ohe and K. Kondo, *Appl. Phys. Lett.*, 1995, **67**, 3895.
16 S. M. Morris, M. J. Clarke, A. E. Blatch and H. J. Coles, *Phys. Rev. E: Stat., Nonlinear, Soft Matter Phys.*, 2007, **75**, 041701.
17 A. E. Blatch, M. J. Coles, B. Musgrave and H. J. Coles, *Mol. Cryst. Liq. Cryst.*, 2003, **401**, 161.
18 M. J. Clarke, A. E. Blatch and H. J. Coles, *Mol. Cryst. Liq. Cryst.*, 2005, **434**, 367.
19 H. Coles, M. Pivnenko and J. Hannington, *WO/2005/075603*, 2005.
20 K. R. Welford and J. R. Sambles, *Mol. Cryst. Liq. Cryst.*, 1987, **147**, 25.
21 M. G. Clark, E. P. Raynes, R. A. Smith and R. J. A. Tough, *J. Phys. D: Appl. Phys.*, 1980, **13**, 2151.
22 D. Meyerhofer, *J. Appl. Phys.*, 1975, **46**, 5084.
23 P. Kassubeck and G. Meier, *Mol. Cryst. Liq. Cryst.*, 1969, **8**, 305.
24 F. Grandjean, *C. R. Acad. Sci.*, 1920, **172**, 71.
25 R. Cano, *Bull. Soc. Fr. Mineral. Cristallogr.*, 1967, **90**, 333.
26 M. Hird, *Chem. Soc. Rev.*, 2007, **36**, 2070.